# 0.3V Bulk-Driven Current Conveyor

## FABIAN KHATEB [1,2], TOMASZ KULEJ [3], AND MONTREE KUMNGERN[4]

[1]Department of Microelectronics, Brno University of Technology, 601 90 Brno, Czech Republic
[2]Faculty of Biomedical Engineering, Czech Technical University in Prague, 272 01 Kladno, Czech Republic
[3]Department of Electrical Engineering, Technical University of Częstochowa, 42-201 Częstochowa, Poland
[4]Department of Telecommunications Engineering, Faculty of Engineering, King Mongkut's Institute of Technology Ladkrabang, Bangkok 10520, Thailand

Corresponding author: Fabian Khateb (khateb@feec.vutbr.cz)

**ABSTRACT** This paper presents the design and the experimental results of a sub 0.5 V bulk-driven (BD) current conveyor (CCII) using 0.18 $\mu$m TSMC CMOS technology with a total chip area of 0.0134 mm$^2$. All transistors are biased in the subthreshold region for low-voltage low-power operation and the input transistors are controlled from their bulk terminals for rail-to-rail input voltage range. The circuit is designed to work with voltage supply ($V_{DD}$ = 0.3V), which is much lower than the threshold voltage of the MOS transistor ($V_{TH}$ =0.5V) while consuming 19 nW of power. The measurement results confirm the proper function of the proposed circuit.

**INDEX TERMS** Bulk-driven, low-voltage, low-power, sub 0.5-V circuits.

## I. INTRODUCTION

Extremely low-voltage (LV) and low-power (LP) CMOS circuits have found a number of applications in contemporary portable and implantable electronic systems. In the last decades, various circuit techniques have been developed to overcome the design constraints associated with LV operation [1]. One of the techniques which attracted considerable attention in recent years depends on the application of subthreshold-biased bulk-driven (BD) MOS transistors, which allows designing circuits supplied with sub 0.5 V supply and rail-to-rail signal swing [2], [3].

The second generation current-conveyor (CCII) is a useful current-mode building block which has found a number of applications in low-voltage systems [4]–[11]. In the last years several low-voltage low-power CCIIs have been presented in the literature, for instance a CCII based on bulk-driven folded cascode OTA with ± 0.4 V voltage supply and 64 $\mu$W power consumption has been presented in [7], a CCII based on floating-gate folded cascode OTA with ± 0.5 V voltage supply and 10 $\mu$W power consumption has been presented in [8], a CCII based on bulk-driven voltage follower with 0.5 V voltage supply and 30 $\mu$W power consumption has been presented in [9], a gate-driven CCII using adaptive biasing technique with ±0.75 V voltage supply and 150 nW power consumption has been presented in [10], a gate-driven subthreshold CCII with 0.4 V voltage supply and 1.8 $\mu$ W power
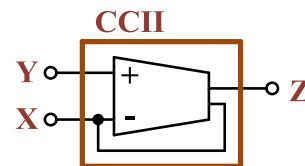
**FIGURE 1.** CCII based on two outputs op-amp.

consumption has been presented in [11]. The performance of the all above mentioned LV LP CCIIs were confirmed by simulation only.

This paper presents a new solution for a LV/LP BD CCII that can operate from $V_{DD}$ of 0.3 V, while consuming only 19 nW of power and offering a rail-to-rail signal swing at the same time. The ultra-low $V_{DD}$ has been achieved thanks to the use of a BD non-tailed differential amplifier. Moreover, the structure shows an improved 3-dB bandwidth of a current gain and can operate without any compensation capacitance, even for large loading capacitances, while offering precise voltage and current gain values at the same time.

The rest of the paper is organized as follows. In section II, the structure of the proposed bulk-driven CCII is described. Section III presents the experimental results. Finally, the conclusions are given in section IV.

## II. BULK-DRIVEN CCII

The proposed positive CCII, as shown in Fig. 1, is based on two outputs op-amp operating in unity-gain feedback configuration that ensure $V_Y = V_X$ and $I_Z = I_X$.
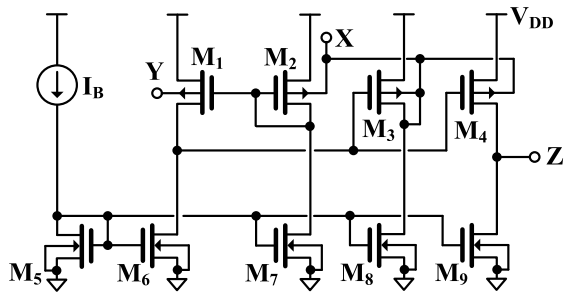
**FIGURE 2.** CMOS schematic of BD-CCII.

The schematic of the proposed CCII is shown in Fig. 2. The circuit consists of a precise Y-X voltage follower ($M_1$-$M_3$, $M_5$-$M_8$) and an additional current repetition circuit ($M_4$, $M_9$), that creates the unity-gain current amplifier and the Z output of the conveyor. The voltage follower was first proposed and validated by simulations in [12]. Let us remind briefly its principle of operation. The circuit can be considered as a simple two-stage op-amp operating in a unity-gain feedback configuration.

Transistors $M_1$ and $M_2$ form a simple non-tailed differential amplifier loaded by the current sinks $M_6$ and $M_7$. The second stage of the internal op-amp is created by the transistor $M_3$ loaded by the current sink $M_8$. The bulk terminals of $M_2$ and $M_3$ are shorted together and connected to the output of the op-amp. Such a connection closes a negative feedback loop, thus creating a unity-gain voltage buffer. Note, that shorting together the bulk terminals of $M_2$ and $M_3$ ensures that the threshold voltages of the two transistors are changing in the same way with the input signal. This improves the accuracy of the voltage gain. Without this connection the internal op-amp would have poor CMRR performance, which would affect the accuracy of the voltage gain of the resulting voltage follower, causing its value to be greater than unity. It is worth mentioning that the CCII can be simply extended to have multiple outputs with both polarities by using the cross-coupled current mirror technique.

The minimum supply voltage of the CCII can be expressed as follows:

$$V_{DDmin} = \max(V_{SG2} + V_{DSsat7}; V_{SG3,4} + V_{DS6}) \quad (1)$$

where $V_{DSsat}$ is the saturation voltage of an MOS transistor. Assuming $V_{SG2,3,4} = V_{DSsat}$ in a weak inversion region the minimum $V_{DD}$ can be as low as $2V_{DSsat}$ (ca. 200 mV). In practical realizations however, the minimum $V_{DD}$ has to be slightly increased due to the process/temperature variations and signal swing. Nevertheless, the minimum $V_{DD}$ is around 1/3 lower as compared to traditional solutions based on long tail differential pairs.

Neglecting the parasitic pole associated with the drain/gate node of $M_2$:

$$\omega_p \approx -\frac{g_{m2}}{C_{gs1} + C_{gs2}} \quad (2)$$

namely assuming that the pole is located well above the gain bandwidth product (GBW) of the internal op-amp, the voltage gain of the follower can be expressed as:

$$A_v(s) = \frac{V_x(s)}{V_y(s)} = A_{vo} \frac{\omega_o^2}{s^2 + s\frac{\omega_o}{Q} + \omega_o^2} \quad (3)$$

where:

$$\omega_o = \sqrt{\omega_1 \omega_2} \quad (4)$$

$$\omega_1 = \frac{1 + g_{m1}r_1}{C_1 r_1} \approx \frac{g_{m1}}{C_1} \quad (5)$$

$$\omega_2 = \frac{g_{mb3} + g_{ds3} + g_{ds8}}{C_x} \approx \frac{g_{mb3}}{C_x} \quad (6)$$

and:

$$Q = \frac{\sqrt{\frac{\omega_1}{\omega_2}}}{1 + \frac{\omega_1}{\omega_2(1 + g_{m1}r_1)}} \quad (7)$$

where $C_1$, $r_1$ are the output capacitance and resistance of the first stage of the op-amp, and $C_x$ is the capacitance of the X terminal.

As it can be concluded from the above equations it is relatively easy to provide stable operation of the follower even for large $C_x$ and without any compensation capacitance inside the feedback loop, which is beneficial for silicon area. The quality factor Q is relatively low for $\omega_1 < \omega_2$, i.e. for small capacitance $C_x$, then it increases with increasing $C_x$ (decreasing $\omega_2$), achieves its maximum for $\omega_2 = \omega_1/(1 + g_{m1}r_1)$, which is equal to $Q_{max} = (1 + g_{m1}r_1)^{1/2}/2$ and then again starts to decrease. Thus, the circuit can operate even for very large $C_x$ without any compensation capacitance, provided that the resulting slew-rate (SR) and $Q_{max}$ will be sufficient for a given application.

The ease of frequency compensation may be attributed to the low open-loop voltage gain of the internal op-amp, which is lowered by the bulk-drain connection of $M_3$.

For $\omega_1 << \omega_2$, the 3-dB frequency of the Y-X follower may be approximated as:

$$f_{3dB} \approx \frac{g_{m1}}{2\pi C_1} \quad (8)$$

Assuming $g_{m1}/g_{mb1} = g_{m2}/g_{mb2}$, the dc voltage gain of the follower can be expressed as:

$$A_{vo} = \frac{A_{eq}}{1 + A_{eq}} \quad (9)$$

where $A_{eq}$ is the voltage gain of an equivalent op-amp operating in a voltage follower configuration, which is given by [12]:

$$A_{eq} = \frac{g_{mb1}}{g_{o1}} \cdot \frac{g_{m3}}{g_{o3}} \cdot \frac{g_{m3} + g_{o3}}{g_{m3} + g_{mb3} + g_{o3}} \quad (10)$$

where $g_{o1} = g_{ds1} + g_{ds6}$ and $g_{o3} = g_{ds3} + g_{ds8}$. As it can be concluded from the above equation, the dc voltage gain of the Y-X follower is close to the voltage gain of the follower based on the unloaded two-stage internal op-amp, despite the drain-bulk connection in $M_3$. Even though the value of $A_{eq}$ is subject to transistor mismatch, the voltage gain error
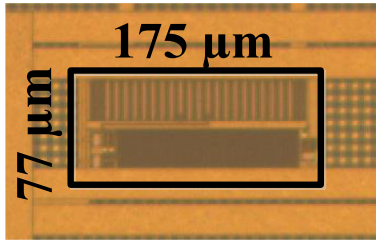
**FIGURE 3.** Chip microphotograph of the proposed BD-CCII.

with respect to unity can be maintained much below 1% for reasonable transistor sizes [12].

The output resistance of the voltage follower (i.e. the resistance $R_x$ of the CCII) can be approximated as:

$$R_x \cong \frac{1}{g_{m3} \frac{g_{mb1}}{g_{o1}}} \tag{11}$$

thus, it is equal to the reciprocal value of the transconductance $g_{m3}$ multiplied by the voltage gain of the input differential amplifier. Since the output resistance of the Z terminal is equal to $R_z = 1/g_{o4}$, where $g_{o4} = g_{ds4} + g_{ds9}$, then the $R_z/R_x$ ratio is given by:

$$\frac{R_z}{R_x} \cong \frac{g_{m3}}{g_{o4}} \cdot \frac{g_{mb1}}{g_{o1}} \tag{12}$$

and can exceed $10^3 \Omega/\Omega$. Given that $V_z = V_x$, the dc current gain $I_z/I_x$ is equal to the ratio of transconductances $g_{m4}/g_{m3}$ and is equal to unity as long as transistor mismatch is not considered.

Another interesting property of the proposed structure of the BD CCII is that the 3-dB frequency of the current amplifier can be much larger than the GBW product of an internal op-amp. This may be attributed to the additional feedforward path from X to Z terminals, through the bulk terminal of $M_4$. Since the bulks of $M_3$ and $M_4$ are shorted together, the two transistors form a BD current mirror which can transfer a current even for frequencies much above the GBW of the internal op-amp. Hence, the 3-dB frequency of the current amplifier for the Z terminal shorted to ground for ac signals and the X input excited with an ideal current source can be approximated as:

$$\omega_i \approx \frac{g_{mb3}}{C_x} \tag{13}$$

where $C_x$ is the total capacitance associated with the X terminal of the CCII.

The input referred thermal noise of the considered CCII is determined by the input noise of the input differential amplifier ($M_1$, $M_2$, $M_6$, $M_7$) and can be approximated as:

$$\overline{v_n^2} = 2 \frac{2nkT}{g_{mb1}^2} \left( g_{m1,2} + g_{m5,6} \right) \tag{14}$$

where n is the subthreshold slope factor (assumed identical for p- and n-channel transistor), k is the Boltzmann constant and T is the temperature.
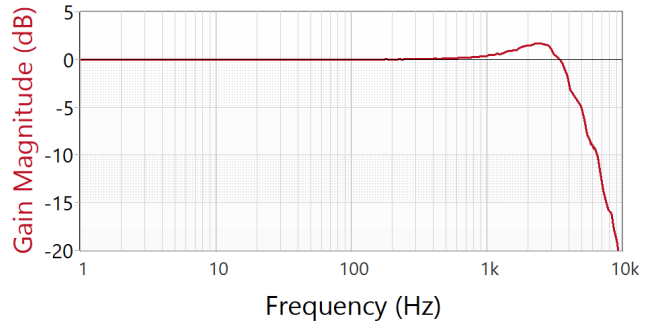


**FIGURE 4.** Measured frequency response of the voltage gain $V_X/V_Y$.
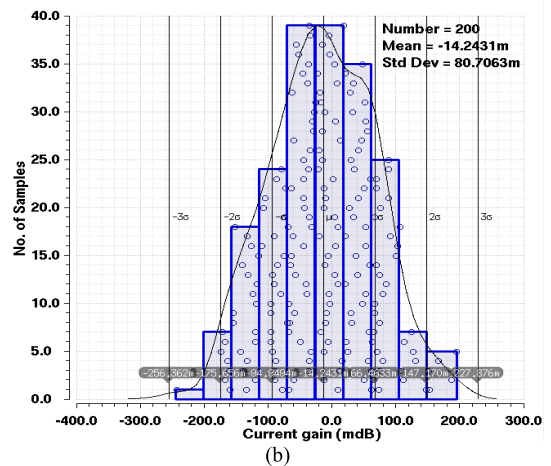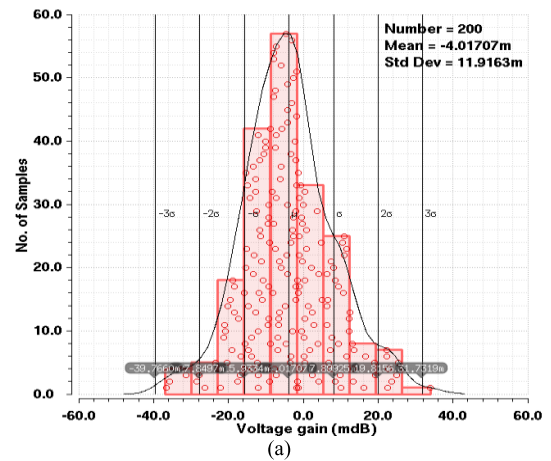


**FIGURE 5.** The histogram of the (a) voltage and (b) current gains @100Hz based on Monte Carlo analysis.

## III. EXPERIMENTAL RESULTS

The proposed BD-CCII has been implemented in a standard 0.18 $\mu$m CMOS process from TSMC ($V_{TH} \approx +/-0.5$ V). The chip microphotograph is shown in Fig. 3 with total chip area of 0.0134 mm$^2$. The circuit was designed for $V_{DD} = 0.3$ V, $I_B = 2.5$ nA, nevertheless it can operate also from larger $V_{DD}$ (up to 0.5 V) and larger biasing currents (up to around 100 nA), which would result in larger bandwidth. The value of the maximum biasing current depends on the $V_{DD}/V_{TH}$ ratio, therefore, using processes with lower $V_{TH}$ the biasing current could be significantly increased.
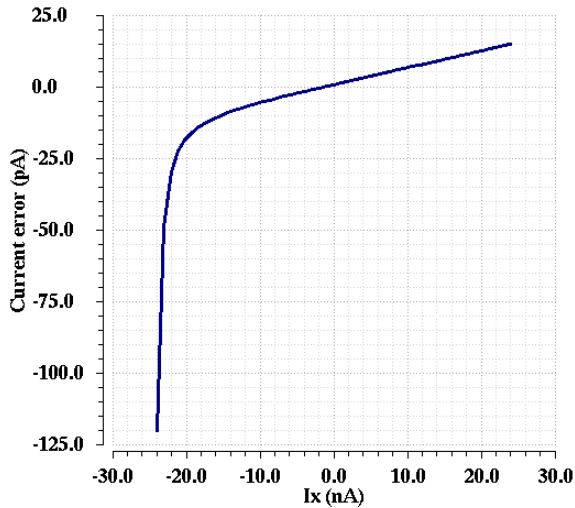
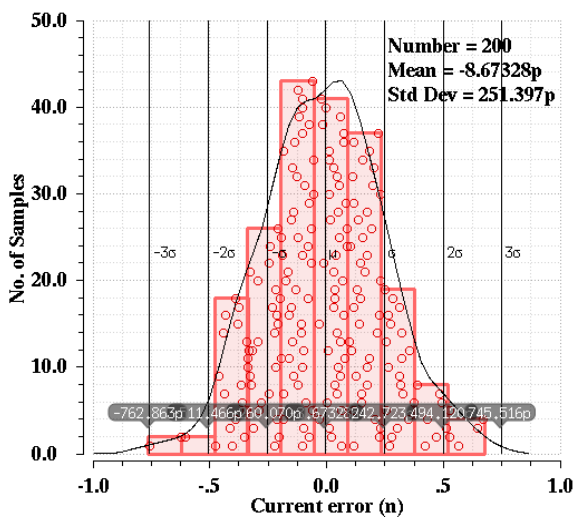**FIGURE 6.** The simulated dc current error versus $I_X$.



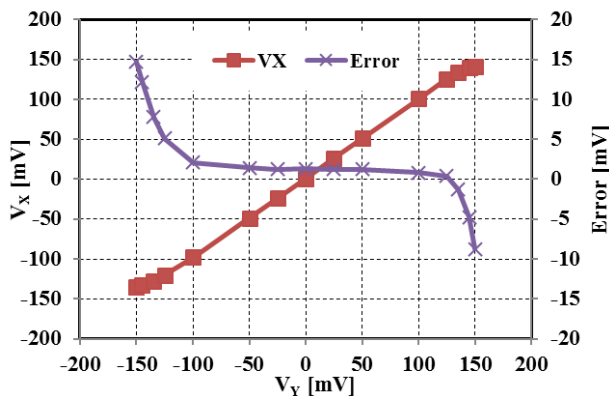**FIGURE 7.** The histogram of the DC current error based on Monte Carlo analysis.



**FIGURE 8.** Measured DC characteristic of the BD-CCII.

**TABLE 1.** Worst-case performances of the BD-CCII over process and temperature corners for $V_{DD}$ =0.3 V, $C_L$ =30 pF.

| Parameter (T=27 ℃) | SS | SF | TT | FS | FF |
|---|---|---|---|---|---|
| Power consumption [nW] | 18.8 | 18.9 | 19 | 19.1 | 19.3 |
| -3dB bandwidth $I_Z/I_X$ [kHz] | 37.66 | 39.18 | 39.2 | 39.29 | 40.99 |
| -3dB bandwidth $V_X/V_Y$ [kHz] | 5.33 | 5.25 | 5.32 | 5.38 | 5.31 |
| Current gain $I_Z/I_X$ [-] | 0.999 | 0.999 | 0.999 | 0.999 | 0.999 |
| Voltage gains $V_X/V_Y$ [-] | 0.999 | 0.999 | 0.999 | 0.999 | 0.998 |

| Parameter (TT corner) | -10º | 27º | 70º |
|---|---|---|---|
| Power consumption [nW] | 18.7 | 19 | 21 |
| -3dB bandwidth $I_Z/I_X$ [kHz] | 44.4 | 39.2 | 36 |
| -3dB bandwidth $V_X/V_Y$ [kHz] | 5.8 | 5.32 | 4.7 |
| Current gain $I_Z/I_X$ [-] | 0.999 | 0.999 | 0.997 |
| Voltage gains $V_X/V_Y$ [-] | 0.998 | 0.999 | 0.991 |
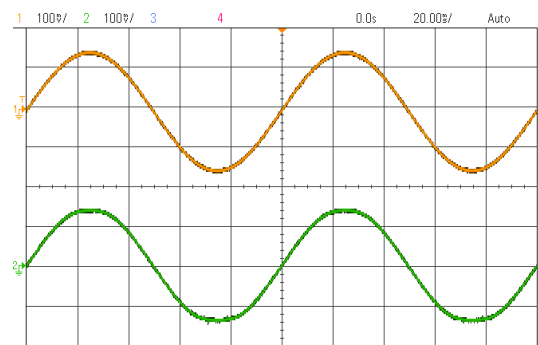


**FIGURE 9.** Measured sine wave responses $V_Y$ and $V_X$ of the CCII for rail-to-rail input and 100 Hz frequency.
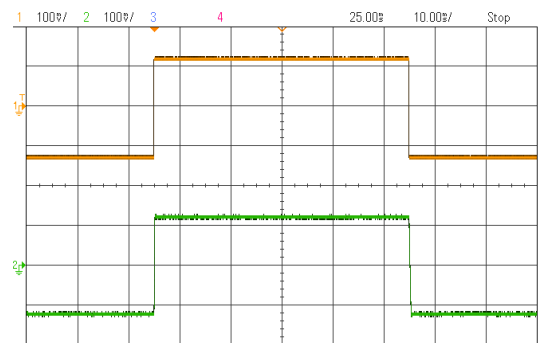


**FIGURE 10.** Measured step responses $V_Y$ and $V_X$ of the CCII with 100 Hz frequency.

$M_4 = 5 \times 50/1$, $M_6$, $M_7 = 100/1$, $M_8$, $M_9 = 5 \times 100/1$. The transistor channel lengths were chosen relatively large in order to decrease their output conductances and consequently improve the accuracy of the dc voltage and current gains and the $R_Z/R_X$ ratio. The W/L ratios are also relatively large, to decrease the $V_{GS}$ voltages of transistors for the given biasing currents, as well as to decrease their flicker noise and offset.

Once the channel lengths were set, the channel widths were determined during the simulation phase to meet the requirement $|V_{GSqi}| \approx V_{DD}/2$, where $V_{GSqi}$ is the quiescent gate-source voltage of the i-th MOS transistor (i=1-9). This ensures the largest voltage headroom for possible

In this design, the biasing current has been adjusted to obtain minimum $V_{DD}$ for the given $V_{TH}$ voltages, while taking into account also the possible process and temperature variations. The load capacitance was 30 pF. The transistor dimensions in $\mu$m/$\mu$m were as follows: $M_1$, $M_2$, $M_5$ = 50/1, $M_3$,

**TABLE 2.** Experimental results of the BD-CCII and compared to others.

| Parameter | This work BD-CCII | | [7] | [8] | [9] | [11] |
|---|---|---|---|---|---|---|
| Supply voltage [V] | 0.3 | 0.5 | ±0.4 | ±0.5 | 0.5 | 0.4 |
| Bias current [nA] | 2.5 | 40 | - | - | - | - |
| Power consumption [nW] | 19 | 509 | 64E3 | 10E3 | 30E3 | 1.8E3 |
| Slew rate SR+ [V/ms] | 2 | 45.2 | - | - | - | - |
| Slew rate SR- [V/ms] | 0.66 | 11.2 | - | - | - | - |
| -3dB bandwidth $I_Z/I_X$ [kHz]* | 39.2 | 578 | 13E3 | 8.2E3 | 10E3 | 1.25E3 |
| -3dB bandwidth $V_X/V_Y$ [kHz] | 4.1 | 56.4 | 14E3 | 4.8E3 | 11E3 | 1E3 |
| Current gain $I_Z/I_X$ [-]* | 0.999 | 0.999 | 1 | 1 | 0.996 | 1 |
| Voltage gains $V_X/V_Y$ [-] | 0.9987 | 0.999 | 1 | 1 | 0.998 | 1.004 |
| Input current range [nA] | ±24 | ±400 | ± 7E3 | ± 3E3 | ± 15E3 | - |
| Input voltage range [mV] | 300 | 500 | ± 380 | ± 500 | 60:460 | - |
| Input thermal noise [$\mu$V/Hz$^{1/2}$]* | 1.9 | 0.5 | - | - | - | - |
| Input referred offset [mV] [a] | 2 | 2 | - | - | - | - |
| Current offset [pA] [a] | 248 | 248 | - | - | - | - |
| Parasitic resistance $R_Y$ [M$\Omega$]* | 703 | 664 | $\approx \infty$ | $\approx \infty$ | $\approx \infty$ | - |
| Parasitic resistance $R_X$ [$\Omega$]* | 56E3 | 3E3 | 27 | 42 | 260 | 106 |
| Parasitic resistance $R_Z$ [M$\Omega$]* | 94.7 | 8 | 0.89 | 53 | 0.113 | - |
| $(V_{TH}/V_{DD})$*100 [%] | 166 | 100 | 62 | 50 | 100 | 87 |
| $(V_{in-max}/V_{DD})$*100 [%] | 100 | | 95 | 100 | 80 | - |
| $C_L$ [pF] | 30 | | - | - | - | - |
| CMOS technology [$\mu$m] | 0.18 TSMC | | 0.18 TSMC | 0.18 TSMC | 0.18 TSMC | 0.09 TSMC |
| Chip area [mm²] | 0.0134 | | - | - | - | - |
| Results | Meas. | | Sim. | Sim. | Sim. | Sim. |

(*) Simulated
[a] standard deviation (MC 200 runs)

process/temperature variations and signal swing. The biasing currents of the input differential amplifier were set to ensure sufficiently low Y input referred thermal noise of the CCII. The proportions of currents $I_{D3}/I_{D1,2}$ were determined to ensure sufficient stability margin for the assumed load capacitance of the X terminal (sufficient value of $g_{mb3}$). For the given W/L ratios the parasitic pole associated with the drain/gate node of $M_2$ was much above the 3-dB frequency of the Y-X voltage follower, hence, its impact was negligible. Finally, the results of MC and noise analyses showed that the assumed transistor channel areas were sufficiently large to provide acceptable levels of input referred flicker noise, offsets and the voltage/current gains accuracies.

Selected post-layout simulation and measured results of the proposed BD-CCII are shown in Figs. 4-10. For the purpose of measurement a symmetrical supply voltage of $+/-0.15$ V was used. Fig. 4 shows the measured magnitude response of the voltage follower ($V_X/V_Y$) using the Vector Network Analyzer Bode 100. The dc voltage gain was -11 mdB (0.9987 V/V), which corresponds to the accuracy provided by a 57.7 dB op-amp operating in a unity-gain feedback configuration. This confirms experimentally, that a high-precision voltage follower can be realized using relatively low voltage gain of the internal op-amp.

The 3-dB cutoff frequency was 4.1 kHz, while the estimated Q factor (see (7)) was around 1.25. Note, that the above results were achieved for relatively large $C_X$ (30 pF) and without any compensation capacitance, that confirms theoretical predictions.

Fig. 5 shows the histogram of the DC voltage and current gains of the CCII based on Monte Carlo analysis (200 runs). The standard deviation was 11.9 mdB and 80.7 mdB for the voltage and current gain, respectively. Note, that the maximum error of a voltage gain was 40 mdB (0.46 %), which is still acceptable in many applications. The maximum error of a current gain was larger and equal to around 2 %.

Fig. 6 shows the simulated DC current error ($I_Z - I_X$) versus the input current $I_X$. The current error was below 18 pA for $I_X$ in range of ±20 nA. Fig. 7 shows the histogram of the DC current error based on Monte Carlo (200 runs). The standard deviation was 251 pA. Figs. 6 and 7 confirm acceptable current tracking accuracy.

Fig. 8 shows the measured DC transfer characteristic of the Y-X voltage follower and the voltage error. The voltage error was ranging from -8.7 mV to 14.6 mV for $V_Y$ ranging from 150 mV to -150 mV respectively (i.e. rail-to-rail).

The measured sine-wave response of the follower with the input sine-wave of 300 mV peak-to-peak value (rail-to-rail)

and 100-Hz frequency is shown in Fig. 9. The THD was below 1% for $V_Y < 246$ mV$_{pp}$.

Fig. 10 shows the measured step response of the BD-CCII when a 250 mV peak-to-peak and 100 Hz square wave was applied to the Y terminal. The slew rate SR+ was 2V/ms and SR- was 0.66 V/ms. The SR was limited mainly by the class A output stage, therefore it is unsymmetrical. This disadvantage could be overcome applying a class AB output stage.

Table 1 shows the worst case performances of the BD-CCII over process and temperature variation. The process corners for MOS transistor were fast-fast (FF), fast-slow (FS), slow-fast (SF) and slow-slow (SS); and the temperature corners were -10 °C, 27 °C and 70 °C. The results in Table 1 confirm the robustness of the design over process and temperature corners.

Table 2 summarizes the measured results of the proposed BD-CCII for $V_{DD} = 0.3$ V and 0.5 V and compare them with other LV LP CCIIs. The proposed BD-CCII offers the lowest voltage supply and power consumption and the highest $V_{TH}/V_{DD}$ and $V_{in-max}/V_{DD}$ ratios. As it was predicted theoretically, the 3-dB bandwidth of the current gain was much larger than the 3-dB frequency of the voltage gain. The input current range was limited by the biasing current of $M_3$ ($M_4$). The thermal noise was dominant for frequencies larger than around 5 Hz. The $R_Z/R_X$ ratio for the considered CCII was around 1.7E3, which seems to be sufficient for many applications. Note, that the larger value of $V_{DD}$ (larger $V_{DD}/V_{TH}$ ratio) allows increasing both, the voltage and the current gain bandwidth, since larger biasing currents are possible. Therefore, applying the low $V_{TH}$ CMOS processes, one could achieve much higher frequency range using the same structure. In such a case also the cascode/self cascode connections could be used, thus further improving the accuracy of the resulting CCII.

Note, that the CCII is suitable to serve in portable or implementable biomedical applications (e.g. filters, oscillators, amplifiers) where the frequency range of the biological signals is from sub-hertz up to 10 kHz and the low-voltage supply low-power consumption are the main demand.

## IV. CONCLUSION

The paper presents the measured results for an ultra-low voltage low-power CCII based on bulk-driven technique. The proposed structure is simple and capable to work with 0.3 V supply while consuming 19 nW of power. The very low minimum $V_{DD}$ was achieved thanks to the application of non-tailed differential stage. The circuit offers good accuracy of the voltage gain with relatively low dc voltage gain of an internal op-amp, which allows neglecting a compensation capacitance even for large capacitance $C_x$. The 3-dB frequency of the current gain is increased due to the additional feedforward path, which is an additional advantage of the proposed structure. The measured results are close to the simulated ones and confirm the attractive features of the proposed circuit.

## REFERENCES

[1] F. Khateb, S. B. A. Dabbous, and S. Vlassis, "A survey of non-conventional techniques for low-voltage low-power analog circuit design," *Radioengineering*, vol. 22, no. 2, pp. 415–427, 2013.

[2] F. Khateb and T. Kulej, "Design and implementation of a 0.3-V differential difference amplifier," *IEEE Trans. Circuits Syst. I, Reg. Papers*, vol. 66, no. 2, pp. 513–523, Feb. 2019. doi: 10.1109/TCSI.2018.2866179.

[3] T. Kulej and F. Khateb, "Design and implementation of sub 0.5-V OTAs in 0.18-$\mu$m CMOS," *Int. J. Circuit Theory Appl.*, vol. 46, no. 6, pp. 1129–1143, 2018.

[4] P. Colucci *et al.*, "CCII-based voltage amplifier optimization for reduced relative gain error," *Circuits, Syst., Signal Process.*, vol. 37, no. 3, pp. 1315–1326, 2018.

[5] V. Stornelli, G. Ferri, L. Pantoli, G. Barile, and S. Pennisi, "A rail-to-rail constant-$g_m$ CCII for instrumentation amplifier applications," *AEU-Int. J. Electron. Commun.*, vol. 91, pp. 103–109, Jul. 2018.

[6] A. De Marcellis, G. Ferri, and P. Mantenuto, "A CCII-based non-inverting Schmitt trigger and its application as astable multivibrator for capacitive sensor interfacing," *Int. J. Circuit Theory Appl.*, vol. 45, no. 8, pp. 1060–1076, 2017.

[7] F. Khateb, N. Khatib, and D. Kubánek, "Novel low-voltage low-power high-precision CCII± based on bulk-driven folded cascode OTA," *Microelectron. J.*, vol. 42, no. 5, pp. 622–631, 2011.

[8] F. Khateb, N. Khatib, and D. Kubánek, "Novel ultra-low-power class AB CCII+ based on floating-gate folded cascode OTA," *Circuits Syst. Signal Process.*, vol. 31, no. 2, pp. 447–464, 2012.

[9] G. Raikos, S. Vlassis, and C. Psychalinos, "0.5 V bulk-driven analog building blocks," *AEU-Int. J. Electron. Commun.*, vol. 66, no. 11, pp. 920–927, 2012.

[10] V. Stornelli *et al.*, "The AB-CCII, a novel adaptive biasing LV-LP current conveyor architecture," *AEU-Int. J. Electron. Commun.*, vol. 79, pp. 301–306, Sep. 2017.

[11] M. A. Eldeeb, Y. H. Ghallab, Y. Ismail, and H. Elghitani, "Low-voltage subthreshold CMOS current mode circuits: Design and applications," *AEU-Int. J. Electron. Commun.*, vol. 82, pp. 251–264, Dec. 2017.

[12] T. Kulej and F. Khateb, "Sub 0.5-V bulk-driven winner take all circuit based on a new voltage follower," *Analog Integr. Circuits Signal Process.*, vol. 90, no. 3, pp. 687–691, 2017.

**FABIAN KHATEB** received the M.Sc. and Ph.D. degrees in electrical engineering and communication and also in business and management from the Brno University of Technology, Czech Republic, in 2002, 2005, 2003, and 2007, respectively. He is currently an Associate Professor with the Department of Microelectronics, Faculty of Electrical Engineering and Communication, Brno University of Technology, and also with the Department of Information and Communication Technology in Medicine, Faculty of Biomedical Engineering, Czech Technical University in Prague. He has authored or coauthored more than 100 publications in journals and proceedings of international conferences. He holds five patents. He has expertise in new principles of designing low-voltage low-power analog circuits, particularly biomedical applications. He is a member of the Editorial Board of *Microelectronics Journal*. He is an Associate Editor of the *Circuits, Systems and Signal Processing*, *IET Circuits, Devices and Systems*, and *International Journal of Electronics*. He is a Lead Guest Editor for a special issue on Low Voltage Integrated Circuits and Systems for Circuits, Systems and Signal Processing, in 2017, the *IET Circuits Devices and Systems*, in 2018, and the *Microelectronics Journal*, in 2019. He is also a Guest Editor for a special issue on Current-Mode Circuits and Systems; Recent Advances, Design, and Applications for the *International Journal of Electronics and Communications*, in 2017.

**TOMASZ KULEJ** received the M.Sc. and Ph.D. degrees (Hons.) from the Gdańsk University of Technology, Gdańsk, Poland, in 1990 and 1996, respectively. He was a Senior Design Analysis Engineer with the Polish Branch of Chipworks, Inc., Ottawa, Canada. He is currently an Associate Professor with the Department of Electrical Engineering, Technical University of Częstochowa, Poland, where he conducts lectures on electronics fundamentals, analog circuits, and computer aided design. He has authored or coauthored more than 60 publications in peer-reviewed journals and conferences. He holds three patents. His current research interest includes analog integrated circuits in CMOS technology, with emphasis to low voltage and low power solutions. He serves as an Associate Editor of the *Circuits Systems and Signal Processing* and *IET Circuits Devices and Systems*. He was also a Guest Editor for the special issues on Low Voltage Integrated Circuits on Circuits Systems and Signal Processing, in 2017, the *IET Circuits Devices and Systems*, in 2018, and the *Microelectronics Journal*, in 2019.

**MONTREE KUMNGERN** received the B.S.Ind.Ed., M.Eng., and D.Eng. degrees from the King Mongkut's University of Technology Thonburi (KMUTT), Bangkok, Thailand, in 1998, 2002, and 2006, respectively, all in electrical engineering. He is currently an Associate Professor with the Faculty of Engineering, King Mongkut's Institute of Technology Ladkrabang. His research interests include analogue electronics, analog and digital VLSI circuits, and nonlinear electronic circuits. He has authored or coauthored more than 150 publications in journals and proceedings of international conferences.

• • •